Scalable Metalized Polyacrylonitrile Fiber as the Current Collector for High-Performance Flexible Supercapacitors on Flexible Circuits

1st Kangwei Liu
Division of Energy and Environment
Tsinghua Shenzhen International Graduate School
Shenzhen, China
liu-kw17@mails.tsinghua.edu.cn

2nd Songyang Su
Division of Energy and Environment
Tsinghua Shenzhen International Graduate School
Shenzhen, China
susy16@mails.tsinghua.edu.cn

3rd Bin Liang
Division of Energy and Environment
Tsinghua Shenzhen International Graduate School
Shenzhen, China
85liangbin@163.com

4th Cheng Yang
Division of Energy and Environment
Tsinghua Shenzhen International Graduate School
Shenzhen, China
yang.cheng@sz.tsinghua.edu.cn

***Abstract*—The broad market prospect of portable electronics and wearable devices is making demands for flexible energy storage device with high capacity density and compatibility of the manufacturing process of flexible printed circuit (FPC). Herein we raise a convenient and high-efficiency technique for high performance flexible supercapacitor devices based on nickel conductive membrane (NCM). The NCM was prepared by two-step method, which involved the sputtering of nickel on polyacrylonitrile (PAN) nanofiber membrane and electrodeposition of more nickel on it. The NCM contributes to enhancing electron transport/collection and releasing the stress generated from cycling. With electrodeposited MnO_2 and PPy, the NCM electrodes displayed high performance (271.6 F/g for NCM@MnO_2 and 175.1 F/g for NCM@PPy), enhanced rate performance and outstanding cycling stability. This kind of electrode is able to be fabricated on FPC conveniently with good flexibility with different packaging methods (cross-finger type and sandwich type). This study may arouse broad interests in developing large scaled flexible power devices.**

Keywords—MnO_2; polypyrrole; flexible device; Ni conductive membrane

I. Introduction

The broad market prospect of portable electronics and wearable devices is making demands for flexible energy storage device with high capacity density and compatibility of the manufacturing process of flexible printed circuit (FPC). [1-4]. Supercapacitors, featured with excellent cycling stability, enhanced rate performance and high power density [5-7], for complementing or even replacing batteries and electrolytic capacitors, have been under intensive study. Due to the pseudocapacitive characteristic, TMO and conductive polymers have been regarded as better choices, compared with conventional low-capacitance carbon materials [5, 6, 8-11]. Recently, researches on electrode materials have been focused on constructing three-dimensional metal conductive scaffolds, especially nickel-based ones. For example, Ni nanotube arrays by a modified ZnO template-assisted method was developed for supercapacitors [8, 11]; Ni nanowire arrays (NNA) structure was used to support $Ni(OH)_2$ nanostructured battery cathodes with superior mechanical flexibility [12] *etc*. However, available technologies are still complicated and may lead to difficulties in practical application. It is important to develop a technology to prepare high-performance and mechanical flexible current collectors, which are cost-effective, highly reproducible and compatible with FPC [13-23].

Herein we raise a facile preparation process for high-performance flexible supercapacitor via a nickel-based conductive membrane (NCM). The preparation route of NCM is fully compatible to industrial production processes, such as electrospinning, magnetron sputtering and electro-deposition, which is cost-effective and can be scale-upped by roll-to-roll processes. Then the NCM was loaded with MnO_2 (NCM@MnO_2) and polypyrrole (NCM@PPy) respectively, which presented a high specific capacitance of 271.6 F/g (2 mV/s) for NCM@MnO_2 and 175.1 F/g (2 mV/s)for NCM@PPy. Besides, the NCM@MnO_2 electrode showed outstanding stability with capacitance retention of 91.9% (5000 cycles). The supercapacitor device assembled by NCM@MnO_2 and NCM@Ppy exhibited good flexibility, which exhibited superior cycle stability with 94.5% capacitance remain (4500 cycles). This electrode can be fabricated on the FPC easily with good flexibility in different packaging methods (cross-finger type and sandwich type). In all, this study may arouse broad interests in developing electrodes for flexible devices on FPC.

II. Experimental Section

A. The preparation of nickel conductive membrane

The nickel conductive membrane (NCM) films were fabricated by a three-step method. Firstly, the PAN nanofiber membranes were obtained by electrospinning. Then, a thin layer of nickel were magnetron sputtered onto PAN nanofiber membrane (PAN@Ni), with a thickness of about 40 nm. The electrospinning was operated at +18 kV and -2 kV with a power supply produced by Beijing Ucalery. Finally, more nickel was electrodeposited on PAN@Ni to form a three-dimensional nickel conductive membrane (NCM). The electrodeposition solution contained 1M $NiSO_4 \cdot H_2O$, 0.17M $NiCl_2 \cdot 6H_2O$, 0.65M H_3BO_3 and 0.2 g/L sodium dodecyl sulfate. The solution was then stirred at 60 °C with a certain

pH value of 4.8, which is adjusted by ammonia. After that the sputtered PAN was connected on an DC power supply with a settled current density of 5 mA/cm^2. After a 10-minute electrodeposition, the obtained NCM was taken out and got clean up.

B. Synthesis of NCM@MnO_2 and NCM@PPy

All chemicals used in this work were purchased from Aladdin without any other treatment. After the obtained NCM is dried, MnO_2 and PPy were Electro-deposited on it respectively. All the deposited were operated in a two electrode system with a Pt foil as counter electrode.

The electrolyte solution for MnO_2 is composed of 0.01 M sodium sulfate and 0.1 M $MnAc_2$. The NCM was connected on an DC power supply with a settled current density of 10 mA/cm^2, with a deposition time of 30 -120 s. Then the obtained NCM@MnO_2 was taken out and got clean up by deionized water. A microbalance was used to measure the mass change after the deposition process. It should be noticed that the drying time should be keep consistent with the drying process after the Ni deposition.

The electrolyte solution for PPy is composed of 18g/L oxalic acid, 6.9 mL/ mL pyrrole monomer. Then same two – electrode system and DC power supply is adopted for electro-polymerization with 10 mA/cm^2. After that, the same treatment process is used to measure the mass loading.

C. Characterizations

A scanning electron microscopy (HITACH S4800) is used to observe the morphologies of the samples, before the samples were put into the sample compartment, a thin Au layer was sputtered on it to make sure a good conductivity. A VMP3 (BioLogic) is used to conducting the electrochemical measurements, with a three-electrode system (working electrode, a Pt foil and a saturated calomel electrode). Device assembling

The devices were assembled in two different packaging type.

A sandwich supercapacitor is assembled on a Cu covered PI film. Firstly, the Cu covered PI film is overlapped by a piece of adhesive tape. After that, the required pattern is drawn by layer, then the sample was immersed in a $FeCl_3$ solution to remove the needless part. The LED, switch cathode tap and anode tap were soldered on the obtained FPC. Finally, the NCM@MnO_2, the glass fibre membrane (soaked with electrolyte solution) and the NCM@PPy were assembled between the two taps by layer-by-layer packaging. The supercapasitor is sealed by adhesive tape.

A cross-finger supercapacitor is manufactured by laser etching and electro-deposition. Firstly, the NCM is etched by laser into a cross-finger pattern. After that, MnO_2 and PPy were electro-deposited on the different side with the same processes we used in section B.

III. Results and Discussions

The Fig. 1 shows the SEM photographs of the samples. As shown in Fig. 1a, the original PAN nanofibers have a diameter distribution varying from 250 nm to 350 nm. Then, a thin layer of nickel were magnetron sputtered onto PAN nanofiber membrane (PAN@Ni). After that, a nickel electrodeposition process was adopted to form a thicker Ni layer on PAN@Ni to ensure that it has excellent electrical conductivity and mechanical strength. The NCM showed excellent mechanical flexibility.

The electro-deposition and electro-polymerization techniques were used to fabricate the positive and negative electrode, respectively. Each fiber was covered homogeneously by MnO_2 after 30 s of electro-deposition as shown in Fig. 1c, indicating uniform and excellent electrical conductivity of the whole electrode film. The NCM@PPy samples can also be observed in Fig. 1d. The cracks in the inset image of the Fig. 1d were induced by the electron beam.

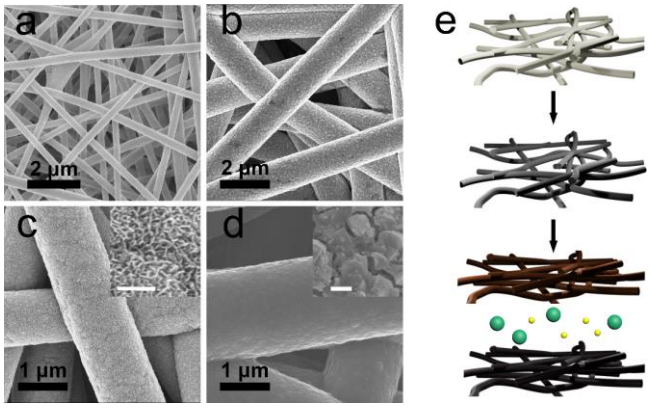

Fig. 1 (a) SEM image of PAN fibers; (b) SEM image of NCM; (c) SEM image of NCM@MnO_2, scale bar of the inset is 200nm; (d) SEM image of NCM@PPy, scale bar of the inset is 500nm; (e) Scheme of the preparation process. From up to bottom: the original PAN (white); the NCM (gray); the NCM@MnO_2 (brown); the electrolyte, sodium ions are shown by yellow balls, sulfate ions are shown by green balls; NCM@PPy (black).

The electrochemical performance of the NCM@MnO_2 electrode was measured in a mild aqueous 0.5 M Na_2SO_4 electrolyte. The mild electrolyte is selected to avoid the NCM getting corrosion. The working potential window was determined in 0 - 0.8 V, wherein the sample exhibited a capacitive behavior and showed no polarization. In the preparation, time is a key factor that decide the mass loading and thickness. With a 120 s deposition process, the mass loading of MnO_2 was up to 0.75 mg cm^{-2}, the NCM@MnO_2 electrode can maintain the standard capacitance property as shown in Fig. 2a. Fig. 2b shows the CV curves of the NCM@MnO_2 at different scan rates. The shape of the curves illustrated that there is no obvious polarization happened even if the scan rate was up to 200 mV s^{-1}, because the special structure of the electro-spun PAN network. The macropores between the PAN fibers give a efficient channels for ion transmission. Furthermore, the Ni layer coated on the PAN fibers also give a highway for electrons. The specific capacitance value of the electrode was calculated as 271.6 F g^{-1} (2 mV s^{-1}). The Fig. 2c shows the GCD curves of the NCM@MnO_2. The result illustrate an excellent rate performance, which exhibited symmetrical charge and discharge processes. Meanwhile, at 5A g^{-1}, the NCM@MnO_2 only exhibited a small IR drop of 0.004 V. the statistics in Fig. 2d also gives a good result in rate performance. When the scan rate was 2 mV s^{-1}, the capacitance was calculated as 271.6 F g^{-1}. When the scan rate achieve 200 mV s^{-1}, the specific capacitance still had 53.8% left (146.2 F g^{-1}), indicating excellent rate performance.

Besides, to further understand the properties NCM@MnO_2, the cycling test by CV and EIS test were operated on an electrochemical station. After a continuous scanning test for 5000 cycles (50 mV s^{-1}), the capacitance retention of the NCM@MnO_2 still remained 91.9%. As shown in Fig. 2f, the EIS analysis of NCM@MnO_2 shows that this system has quick transmission channels. The R_e, which represents electrolyte resistance is calculated as 1.82 Ω, this result shows there exist efficient channels for ion transmission. Meanwhile, the R_{ct}, which represents electron transfer resistance, is calculated as 4.79 Ω. Similar to the electrolyte resistance, the electrons also exhibit quick transmission. In summary, the EIS result illustrate this structure's merit on charge transportation.

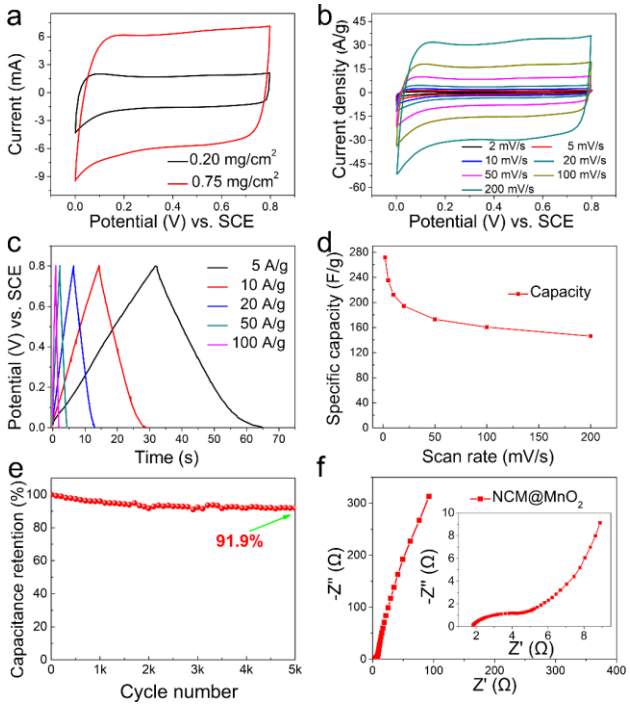

Fig. 2 (a) CV curves of NCM@MnO_2 (0.20 mg cm^{-2} and 0.75 mg cm^{-2})at 50 mV s^{-1}; (b) CV curves of NCM@MnO_2 (0.20 mg cm^{-2}), with the scan rates of 2-200 mV s^{-1}; (c) GCD curves of NCM@MnO_2 at different current densities; (d) The specific capacitance of NCM@MnO_2 at different scan rate; (e) capacitance retention of NCM@MnO_2 at 50 mV s^{-1}; (f) Nyquist plots of the EIS for NCM@MnO_2 with a magnification of the high-frequency region is provided in the inset.

The excellent cycle stability and enhanced specific capacitance feature can be attributed to this factors: Firstly, the highly interconnected 3D NCM structure can effectively decrease the contact resistance so that the NCM exhibited highly conductive feature. Secondly, the macroporous and mesoporous structure of NCM can benefit the ion transport for freely accessing to the interior and exterior surface of the membrane and shuttling across the whole electrode area. Finally, the submicron size of PAN fibers made a critical contribution to high specific surface area for high mass loading of the active materials.

To verify the performance of the NCM more deeply, PPy was chosen as the negative electrode materials to cover NCM via electro-polymerization. CV and GCD tests were operated on a electrochemical station. The working potential window was determined in the range of -0.8 V - 0 V. The mass loading of PPy was controlled to be 0.37 mg cm^{-2}, by electro-polymerizing for 3 min. As shown in Fig. 3,the CV curves of the NCM@PPy electrode at scan rates ranging from 2-200

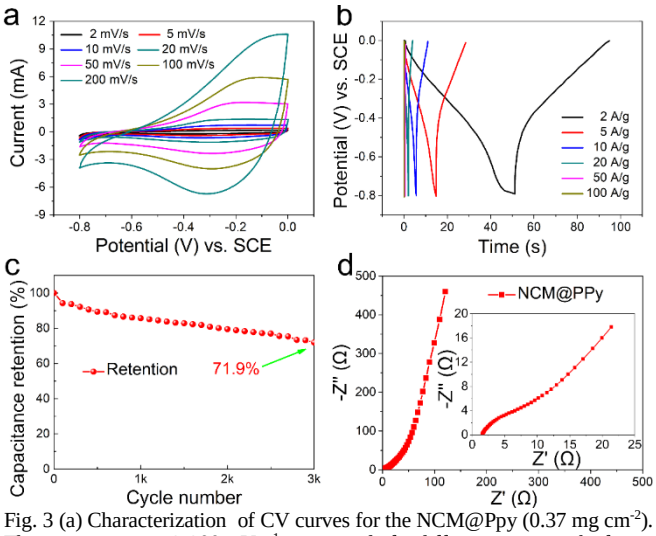

Fig. 3 (a) Characterization of CV curves for the NCM@Ppy (0.37 mg cm^{-2}). The scan rates were 2-200 mV s^{-1} respectively for different curves in the figure; (b) the different curves shows the GCD results (from 2 to 100 A g^{-1}) of the NCM@PPy; (c) the plot and the points gives a statistics of the capacitance change of NCM@PPy in a long time test at 50 mV s^{-1}; (d) EIS results of the NCM@PPy. The inset figure represents the high-frequency region).

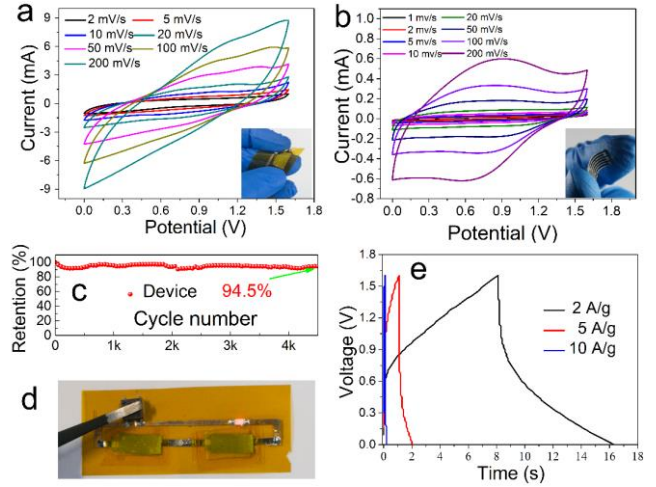

Fig. 4 (a) Characterization of CV curves for the sandwich device (total mass loading of 2.67 mg). The scan rates were 2-200 mV s^{-1} respectively for different curves in the figure; (b) Characterization of CV curves for the cross-finger device (total mass loading of 0.23 mg). The scan rates were 1-200 mV s^{-1} respectively for different curves in the figure; (c) the plot and the points gives a statistics of the capacitance change of sandwich device in a long time test at 50 mV s^{-1}; (d) The assembled supercapacitor could light up a LED lamp. (e) the different curves shows the GCD results (from 2 to 100 A g^{-1}) of the sandwich device.

mVs^{-1} are shown in Fig. 3a. In the meantime, the NCM@PPy gave a specific capacitance of 175.1 F g^{-1} (2 mV s^{-1}). Fig. 3b shows the GCD tests of the NCM@PPy in the range of 2-100 A g^{-1}. Fig. 3c gives a characterization of the long-term stability of the NCM@PPy. After 3000 cycles at 50 mV s^{-1}, 71.9% remained compared with the original capacitance. According to the EIS analysis of NCM@PPy electrode in Fig. 3d, the R_e and R_{ct} of NCM@PPy are 1.53 Ω and 7.49 Ω, respectively.

In order to evaluate the feasibility of the NCM working in a device level, we further assembled flexible sandwich and cross-finger supercapacitors. The sandwich device is assembled on a piece of Cu coated PI film, which is etched as a circuit beforehand. In the meantime, the cross-finger device is manufactured by laser etching and electro-deposition. The as-obtained supercapacitors could work well with a highest potential of 1.6 V. Fig. 4a and 4b describe the CV curves of the devices, respectively giving a capacity of 132.2 Fg^{-1} and 112.1 Fg^{-1} for sandwich device and cross-finger device. Fig.

4e shows typical GCD results of the sandwich device, illustrating pseudocapacitance. Besides, the device retains 94.5% capacitance retention after cycling for 4500 times at the scan rate of 50 mV s^{-1}, indicating the excellent cycling life. The sandwich device was assembled on the FPC, with the taps were fixed on the circuit by solder in advance, as shown in Fig. 4d. with two devices connected in series, a red LED is lighted. Finally, the supercapacitor exhibits a maximum energy density of 1.72 Wh kg^{-1} at the power density of 760 W kg^{-1}, respectively.

IV. Conclusions

In summary, we have demonstrated the controllable preparation of a 3D highly interconnection nickel conductive membrane based on electrospinning, magnetron sputtering and electrodeposition techniques, and systematically investigated its application as electrode scaffold for flexible and high-performance supercapacitors. Combining the flexibility of the PAN membrane and the high conductivity of the Ni layer, the NCM exhibited as an excellent current collector which can well enhance the rate and cyclic performance. The NCM@MnO_2 delivered outstanding capacity (271.6 F g^{-1} at 2 mV s^{-1}) and superior longevity (91.9% capacity retention after 5000 cycles at 50 mV s^{-1}). The devices based on the NCM exhibited high energy density and excellent cycling stability (94.5% capacitance retention after 4500 cycles). This technology can be used to fabricate different kinds of packaging types on FPC (cross-finger type and sandwich type). We believe that the unique structure, high electrochemical performance and mechanical flexibility of this NCM serving for supercapacitor ensure it a promising electrode scaffold for next generation energy storage devices.

Acknowledgment

The authors thank the Local Innovative and Research Teams Project of Guangdong Pearl River Talents Program (2017BT01N111), Shenzhen Geim Graphene Center, the National Nature Science Foundation of China (Project Nos. 51578310), Guangdong Province Science and Technology Department (Project No. 2015A030306010), and Shenzhen Government (Project Nos. JCYJ20170412171430026& JSGG20170414143635496& JSGG20160607161911452) for financial supports.

References

[1] J. Chmiola, C. Largeot, P.-L. Taberna, P. Simon and Y. Gogotsi, "Monolithic carbide-derived carbon films for micro-supercapacitors," science, vol. 238, pp. 480-484, March 2010.

[2] Z. Jiang, Y. Wang, S. Yuan, L. Shi and N. Wang, "Ultrahigh‐working‐frequency embedded supercapacitors with 1T phase $MoSe_2$ nanosheets for system‐in‐package application," Adv. Funct. Mater., vol. 23, p. 1807116, Feb 2019.

[3] B. Xie, Y. Wang, W. Lai, W. Lin and Z. Lin, "Laser-processed graphene based micro-supercapacitors for ultrathin, rollable, compact and designable energy storage components, " Nano Energy, vol. 26, pp. 276-285, Aug 2016.

[4] J. Liu, C. Yang, H. Wu, Z. Lin and Z. Zhang, "Future paper based printed circuit boards for green electronics: fabrication and life cycle assessment," Energy Environ. Sci., vol. 7, pp. 3674-3682, August 2014.

[5] Z. Su, C. Yang, B. Xie, Z. Lin and Z. Zhang, "Scalable fabrication of MnO_2 nanostructure deposited on free-standing ni nanocone arrays for ultrathin, flexible, high-performance micro-supercapacitor," Energy Environ. Sci., vol. 7, pp. 2652-2659, May 2014.

[6] Y. Li, J. Xu, T. Feng, Q. Yao and J. Xie, "Fe_2O_3 nanoneedles on ultrafine nickel nanotube arrays as efficient anode for high-performance asymmetric supercapacitors," Adv. Funct. Mater., vol. 27, p. 1606728, March 2017.

[7] Y. Wang, W. Lai, N. Wang, Z. Jiang and X. Wang, "Reduced graphene oxide/mixed-valent manganese oxides composite electrode for tailorable and surface mountable supercapacitors with high capacitance and super-long life," Energy Environ. Sci., vol. 10, pp. 941-949, February 2017.

[8] D. Chao, X. Xia, C. Zhu, J. Wang and J. Liu, "Hollow nickel nanocorn arrays as threedimensional and conductive support for metal oxides to boost supercapacitive performance," Nanoscale, vol. 6, pp. 5691-5697, March 2014.

[9] S. W. Kim, I. H. Kim, S. I. Kim and J. H. Jang, "Nickel hydroxide supercapacitor with atheoretical capacitance and high rate capability based on hollow dendritic 3D-nickel current collectors," Chem. Asian J., vol. 12, pp. 1291-1296, May 2017.

[10] Z. Sun, S. Firdoz, E. Y. Yap, L. Li and X. Lu, "Hierarchically structured MnO_2 nanowires supported on hollow ni dendrites for high-performance supercapacitors," Nanoscale, vol. 5, pp. 4379-4387, March 2013.

[11] G. Chen, X. Li, L. Zhang, N. Li and T. Y. Ma, "A porous perchlorate-doped polypyrrole nanocoating on nickel nanotube arrays for stable wide-potential-window supercapacitors," Adv. Mater., vol. 28, pp. 7680-7687, Septemper 2016.

[12] C. Xu, J. Liao, C. Yang, R. Wang and D. Wu, "An ultrafast, high capacity and superior longevity ni/zn battery constructed on nickel nanowire array film," Nano Energy, vol. 30, pp. 900-908, December 2016.

[13] W. Lai, Y. Wang, X. Wang, A. Nairan and C. Yang, "Fabrication and engineering of nanostructured supercapacitor electrodes using electromagnetic fields-based techniques," Adv. Mater. Tech., vol. 3, p. 1700168, October 2018.

[14] Y. Wang, W. Lai, Z. Jiang and C. Yang, "All-printed paper based surface mountable supercapacitors," IEEE Transactions on Dielectrics and Electrical Insulation, vol. 24, pp. 676-681, April 2017.

[15] C. Xu, J. Liao, R. Wang, P. Zou and R. Wang, "MoO_3@Ni nanowire array hierarchical anode for all-metal-oxide asymmetric supercapacitors with high capacity and superior longevity," RSC Adv., vol. 6, pp. 110112-110119, November 2016.

[16] J. Liao, X. Wang, Y. Wang, S. Su and A. Nairan, "Lavender-like cobalt hydroxide nanoflakes deposited on nickel nanowire arrays for high-performance supercapacitors," RSC Adv., vol. 8, p. 17263, May 2018.

[17] W. Lai, Y. Wang, Z. Lei, R. Wang and Z. Lin, "High performance, environmentally benign and integratable Zn//MnO_2 microbatteries," J. Mater. Chem. A, vol. 6, pp. 3933-3940, January 2018.

[18] J. Liu, C. Yang, P. Zou, R. Yang and C. Xu, "Flexible copper wires through galvanic replacement of zinc paste: a highly cost-effective technology for wiring flexible printed circuits," J. Mater. Chem. C, vol. 3, pp. 8329-8335, July 2015.

[19] B. Xie, C. Yang, Z. Zhang, P. Zou and Z. Lin, "Shape-Tailorable Graphene-Based Ultra-High-Rate Supercapacitor for Wearable Electronics," Acs Nano, vol. 9, no. 6, pp. 5636-5645, Jun 2015.

[20] H. Tang, C. Yang, Z. Lin, Q. Yang and F. Kang, "Electrospray-deposition of graphene electrodes: a simple technique to build high-performance supercapacitors," Nanoscale, vol. 7, no. 20, pp. 9133-9139, 2015 2015.

[21] Liao, J., Zou, P., Su, S., Nairan, A., Wang, Y., Hierarchical nickel nanowire@$NiCo_2S_4$ nanowhisker composite arrays with a test-tube-brush-like structure for high-performance supercapacitors. J. Math. Chem. A, vol. 6, pp. 15284-15293,June 2018.

[22] Zang, X., Zhang, R., Zhen, Z., Lai, W., Yang, C. and Kang, F., Flexible, temperature-tolerant supercapacitor based on hybrid carbon film electrodes[J]. Nano Energy, vol. 40, pp. 224-232, 2017 August.

[23] Wu, H., Chiang, S. W., Lin, W., Yang, C., Li, and Wong, C. P. Towards practical application of paper based printed circuits: capillarity effectively enhances conductivity of the thermoplastic electrically conductive adhesives[J]. Sci. Rep., vol. 4, pp. 6275, 2014 August.